Chinese Chemical Letters 34 (2023) 107729

Contents lists available at ScienceDirect

Chinese Chemical Letters

journal homepage: www.elsevier.com/locate/cclet

Organoborane cyclophanes with flexible linkers: Dynamic coordination and photo-responsive fluorescence

Zengming Fan, Wenting Sun, Yue Yang, Jiaxiang Guo, Chuandong Dou*, Yue Wang

State Key Laboratory of Supramolecular Structure and Materials, College of Chemistry, Jilin University, Changchun 130012, China

ARTICLE INFO

Article history:
Received 2 June 2022
Revised 26 July 2022
Accepted 5 August 2022
Available online 10 August 2022

Keywords:
Cyclophane
Organoborane
Macrocycle
Coordination
Photo-responsive fluorescence

ABSTRACT

Stimuli-responsive macrocycles are of importance for synthetic chemistry and smart materials. In this manuscript, we report two novel organoborane cyclophanes, which were successfully synthesized by ruthenium-catalyzed olefin metathesis. They are composed of one/two boron-doped helicene π-skeletons and flexible alkyl chain linkers, thus representing a new kind of non-conjugated organoborane macrocycles. Their cyclic structures and photophysical properties, as well as Lewis acidity were theoretically and experimentally investigated. Notably, two enantiomers in one single crystal are observed for one organoborane cyclophane, owning to the presence of helical π-framework in its cyclic structure. Moreover, their Lewis acid-base adducts may dissociate in the excited state and thus display intriguing photo-responsive fluorescence properties, which can be further modulated by temperature. This study thus provides a novel design strategy for non-conjugated organoborane macrocycles, which may promote the development of stimuli-responsive macrocyclic materials with fascinating properties.

Organic macrocycles are an attractive class of compounds owning to not only their unique cyclic structures but also potential utility in the fields of supramolecular assembly, host-guest chemistry, molecular separation, catalysis, *etc.* [1–3]. Increasing attention has been paid to stimuli-responsive macrocycles, which may respond to external stimuli, such as light, heat, pressure and chemical species accompanied with specific functions. Till now, a variety of stimuli-responsive macrocycles containing functional building blocks have been dramatically developed as new smart materials [4–8]. Nevertheless, stimuli-responsive macrocycles remain highly demanded for achieving structural diversity and tailored responsive functions of organic materials.

Because of the unique vacant p-orbital on the boron atom, boron-containing conjugated π-systems exhibit fascinating optical and electronic properties, making them promising candidates as organic optoelectronic materials [9–14]. Tricoordinate organoboranes also have the intriguing Lewis acidity and can bind with Lewis bases to afford tetracoordinate organoboranes, which can be employed to construct stimuli-responsive materials [15–18]. Typically, it has been reported that organoborane-based Lewis acid-base adducts display photo-responsive dissociation behavior in the excited state and thus unique fluorescence properties [19,20]. We recently reported boron-containing organic diradicaloids, which could coordinate with Lewis bases to produce Lewis adducts. As a result, dynamic modulations of (anti)aromaticity and diradical character of organic diradicaloids were unprecedentedly achieved, and furthermore, supramolecular diradicaloids were developed [21,22]. On the other hand, boron-containing macrocycles represent an emerging kind of cyclic molecular system [23–25]. Fig. 1a shows several representative examples, including hexaboracyclophane **1** [26], B–N-doped cycloparaphenylene **2** [27] and block-type B/N-doped cyclophane **3** [28], all of which possess the fully conjugated macrocyclic frameworks and interesting optical and electronic properties, as well as Lewis acidity. For instance, hexaboracyclophane **1** with 2,4,6-tris(trifluoromethyl)phenyl groups on the boron atoms displays high electron-deficiency and extensively delocalized lowest unoccupied molecular orbital (LUMO). In addition, non-conjugated macrocycles with the flexible linkers have weak structural restriction, which provides the potential to modulate intermolecular and intramolecular interactions and thus properties [29]. Therefore, we would like to construct boron-containing non-conjugated macrocycles and exploration of their fascinating structures and properties.

Herein, we report two novel organoborane cyclophanes **4** and **5**, which were successfully synthesized by ruthenium-catalyzed olefin metathesis. They are composed of one/two boron-doped helicene π-skeletons and flexible alkyl chain linkers, thus representing a new kind of non-conjugated organoborane macrocycles. Their cyclic structures and photophysical properties, as well as Lewis

* Corresponding author.
E-mail address: chuandong@jlu.edu.cn (C. Dou).

https://doi.org/10.1016/j.cclet.2022.08.009
1001-8417/

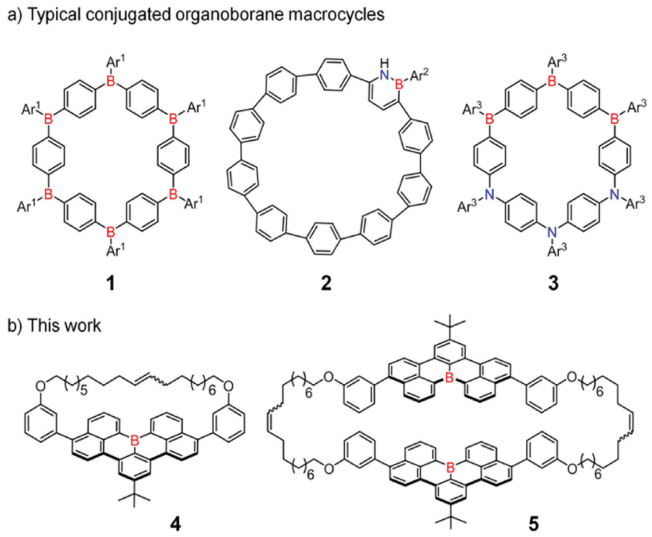

Fig. 1. (a) Typical examples of previously reported conjugated organoborane macrocycles (**1**–**3**). (b) Chemical structures of organoborane cyclophanes (**4** and **5**) in this work.

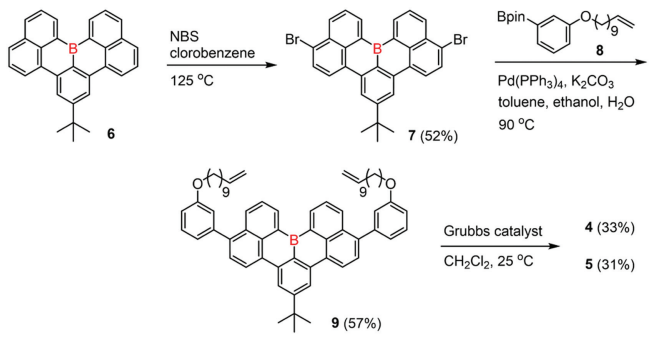

Scheme 1. Synthesis of organoborane cyclophanes **4** and **5**.

acidity were theoretically and experimentally investigated. Notably, two enantiomers in one single crystal are observed for organoborane **4**, owning to the presence of helical π-framework in its cyclic structure. Moreover, their Lewis acid-base adducts may dissociate in the excited state and thus display intriguing photo-responsive fluorescence properties, which can be further modulated by temperature.

In conceiving the synthesis of organoborane cyclophanes, we envisioned that dibromo-containing conjugated organoborane are very crucial to construct macrocyclic structure [29]. Thus, we opted for a stable B-doped helicene as this key building block, which has been first reported by Schickedanz's group [30] and Miyamoto's group [31], respectively. In the previous report, bromination of this molecule occurred at the central benzene ring of the bay region, affording a mono-brominated derivative [30]. To block this bromination mode and obtain double bromination, we first incorporate a *t*-butyl group into this B-doped helicene (Scheme 1). Using Hatakeyama's synthetic method, we successfully synthesized **6** in 30% yield. Bromination of **6** with N-bromosuccinimide (NBS) produced the key dibrominated product **7** in 52% yield, which was subsequently used to perform the Suzuki–Miyaura cross-coupling with **8**, affording the precursor **9** in good yield. Finally, the ruthenium catalyzed olefin metathesis of **9** produced organoborane cyclophanes **4** and **5** containing one or two B-doped helicene moieties in moderate yields, respectively. Their chemical structures were fully characterized by NMR spectroscopy and high-resolution mass spectrometry (HRMS). The HRMS spectra of **4** and **5** show

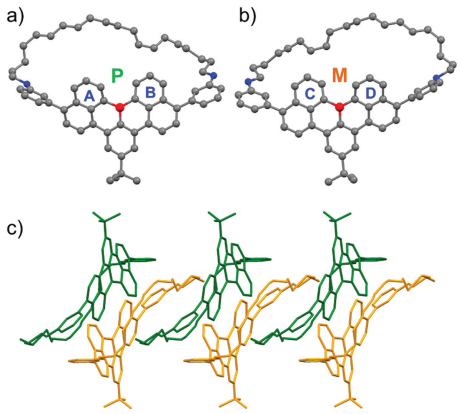

Fig. 2. Single-crystal structures of (a) **4-P** and (b) **4-M**. Hydrogen atoms are removed for clarity. (c) Packing structures of **4**, in which two enantiomers **4-P** and **4-M** are shown in green and orange, respectively.

the clear isotopic distributions, which agree well with their simulated patterns, thus confirming their molecular formulas (Fig. S1 in Supporting information).

The single crystals of organoborane **4** suitable for X-ray crystallographic analysis were fortunately grown by vapor diffusion of *n*-heptane into its CH_2Cl_2 solution. As shown in Fig. 2, two enantiomers **4-P** and **4-M** with the 1:1 ratio in its crystal structure are observable, which are due to the presence of cove region in the B-doped π-skeleton. Both of them exhibit the macrocyclic structures with the dihedral angle of 28.1° for two terminal six-membered rings in the cove region of B-doped π-skeleton. The B–C bond lengths are in the range of 1.539–1.561 Å, which are comparable to that of the pristine B-doped helicene. This comparison suggests that there is negligible strain in the macrocycle with the flexible linker. In the packing structure, two enantiomers **4-P** and **4-M** form one dimer with an upside-down arrangement *via* the weak intermolecular C–H···π interactions, which further stack into tube-type 1D structures (Fig. S2 in Supporting information). There are no π–π interactions in the molecular packing structure. For organoborane **5**, we could not obtain its single crystals for structural analysis after performing various conditions.

Fig. 3a shows the UV-vis absorption spectra and fluorescence spectra of macrocycles **4** and **5** in toluene solutions and neat films (Table 1). In the solutions, **4** and **5** exhibit similar absorption and fluorescence spectra, with the main absorption band (λ_{abs}) at 481 nm and fluorescence maximum (λ_{em}) of *ca.* 510 nm. In thin films, while the absorption curves are slightly red-shifted, the fluorescence spectra are significantly broadened and red-shifted with the λ_{em} of 539 nm for **4** and 545 nm for **5**. The fluorescence quantum yields (Φ_F) of their solutions and films are 0.67/0.16 for **4** and 0.70/0.50 for **5**. These spectral changes are attributed to the molecular aggregation in the film state. From solution to film, in comparison to **4**, **5** has the moderately decreased Φ_F, indicating that the macrocyclic modes impact on the emission properties of non-conjugated macrocycles. Their fluorescence spectra in various solutions show the small solvent effects (Figs. S3 and S4, and Tables S1 and S2 in Supporting information).

To illustrate the absorption spectra of **4** and **5**, we performed time-dependent density functional theory (TD-DFT) calculations at the B3LYP/6–311G(d) level (Fig. 3b and Figs. S9–S11 in Supporting information). The flexible linkers of **5** are simplified to six-carbon alkylenes for calculation (Tables S3 and S4 in Supporting information). The calculated molecular orbitals for **4** and **5′** are fully delocalized on the B-doped helicene. For **4**, the intense absorption is attributed to the HOMO→LUMO transition, accompanied with the calculated wavelength of 477 nm and oscillator strength of 0.4677.

Table 1
Summary of photophysical properties and Lewis acidity of **4** and **5**.

	λ_{abs} (nm) [a]	ε_{max} (L mol^{-1} cm^{-1}) [a]	λ_{em} (nm) [a]	Φ_{em} [a]	λ_{abs} (nm) [b]	λ_{em} (nm) [b]	Φ_{em} [b]	K ($\times 10^5$) [c]
4	481/333	4.03×10^4	511	0.67	488/334	539	0.16	5.55 ± 0.20
5	481/334	6.67×10^4	512	0.70	487/334	545	0.50	7.0 ± 0.77, 3.50 ± 0.11

[a] Measured in toluene solution.
[b] Measured in thin film.
[c] The binding constant of **4**/**5** toward DMAP.

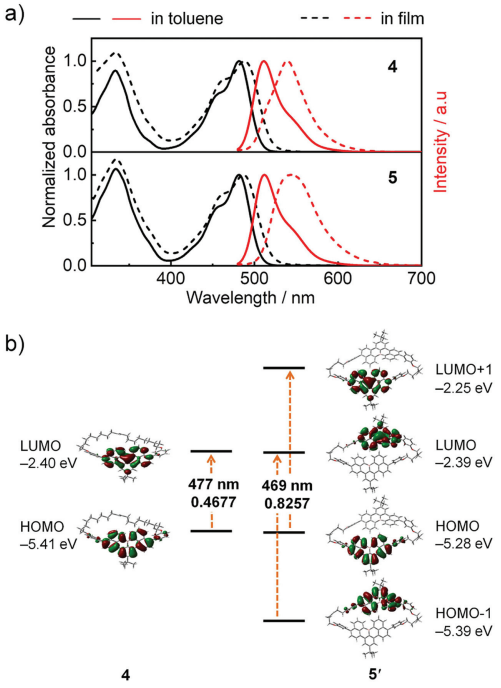

Fig. 3. (a) UV–vis absorption (black) and fluorescence spectra (red) of **4** and **5**. (b) Selected Kohn–Sham molecular orbitals and energy diagrams of **4** and **5′** calculated at the B3LYP/6-311G(d) level, along with theoretical wavelengths and oscillator strengths.

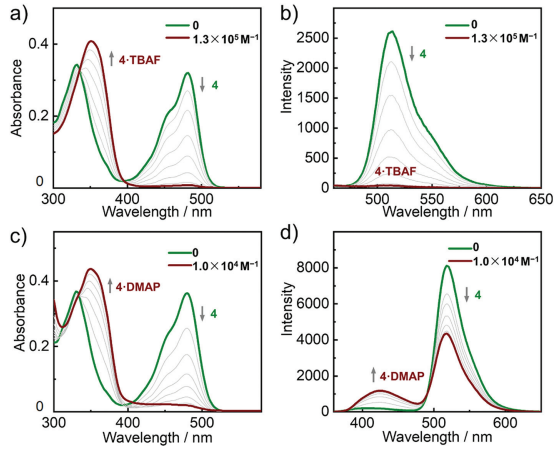

Fig. 4. Titrations of **4** in THF (1×10^{-5} mol/L) with TABF and DMAP monitored by UV-vis absorption (a, c) and fluorescence spectroscopies (b, d).

For **5**, the absorption band is ascribed to the HOMO→LUMO+1 and HOMO−1→LUMO transitions with the similar wavelength but higher oscillator strength. These calculated absorption parameters agree well with their experimental absorption spectra.

To evaluate the Lewis acidity of these organoborane cyclophanes, we carried out titration experiments and monitored the coordination process using UV-vis absorption and fluorescence spectroscopies. Upon addition of tetrabutylammonium fluoride (TBAF) to the THF solution of **4**, while the absorption band at 481 nm for **4** gradually decreased, a new absorption band at 350 nm appeared and increased (Fig. 4). In the fluorescence spectra, the gradual decreases and final disappearance of the emission band around 515 nm for **4** were observed. These spectral changes suggest the formation of **4·TBAF** due to the Lewis acid-base coordination between **4** and TABF. The low fluorescence intensity of **4·TBAF** is probably due to its inhibited conjugation and ionic structure. The binding constant is estimated to be $k = (6.95 \pm 0.97) \times 10^6$ (Fig. S6 in Supporting information). When adding a weaker Lewis base, 4-dimethylaminopyridine (DMAP), the solution of **4** exhibited the similar absorption spectral changes, confirming the binding constant of $k = (5.55 \pm 0.20) \times 10^5$ (Fig. S7 in Supporting information). Notably, the fluorescence spectra changed in a different progress, in which the emission band around 515 nm for **4** gradually decreased and the fluorescence band around 420 nm for **4·DMAP** slowly enhanced, leading to a remarkable dual fluorescence. For **5**, the absorption and fluorescence spectral changes were similar to that of **4**, respectively, and dual fluorescence was also observed in the coordination progress based on DMAP (Figs. S5 and S8 in Supporting information). It has been reported that the Lewis acid-base adducts with modest coordination ability could undergo photodissociation in the excited state to achieve photochromism properties [19,20]. Hence, similar photodissociation behavior should occur for the Lewis adducts based on these organoborane cyclophanes.

To gain insight into the photodissociation behavior of the Lewis adducts, we measured temperature-dependent absorption and fluorescence spectra and time-resolved fluorescence spectra of **4** in the presence of excess DMAP. As shown in Fig. 5a, at 253 K, the absorption spectrum with the band at 350 nm fully originated from **4·DMAP**. With increasing the temperature to 333 K, a small amount of **4·DMAP** in solution dissociated, accompanied with the appearance of the absorption band for **4**. In the fluorescence spectrum at 253 K, two intensive emission bands around 515 and 420 nm were shown, which are ascribed to **4·DMAP** and **4**, respectively (Fig. 5b). When enhancing the temperature, the emission band of **4·DMAP** significantly decreased, whereas the fluorescence band of **4** greatly intensified. These changes demonstrate that high temperature can facilitate the Lewis adducts to dissociate upon photo stimuli. Fig. 5c exhibits the time-resolved fluorescence spectra. After photo excitation, the weak emission bands around 420 nm for **4·DMAP** and 515 nm for **4** simultaneously appeared. Subsequently, while the short-wavelength emission started to weaken and disappeared completely, the long-wavelength emission obviously increased and persisted for several nanoseconds. All of these results reveal that photoexcitation promotes **4·DMAP** to partially dissociate into **4*** in the excited state, thus producing the dual fluorescence from both of **4·DMAP*** and **4*** (Fig. 5d) [19,20].

In conclusion, we synthesized two organoborane cyclophanes **4** and **5** by ruthenium-catalyzed olefin metathesis, which are composed of one/two boron-doped helicene π-skeletons and flexible alkyl chain linkers. We fully investigated their cyclic structures and photophysical properties, as well as Lewis acidity. Notably,

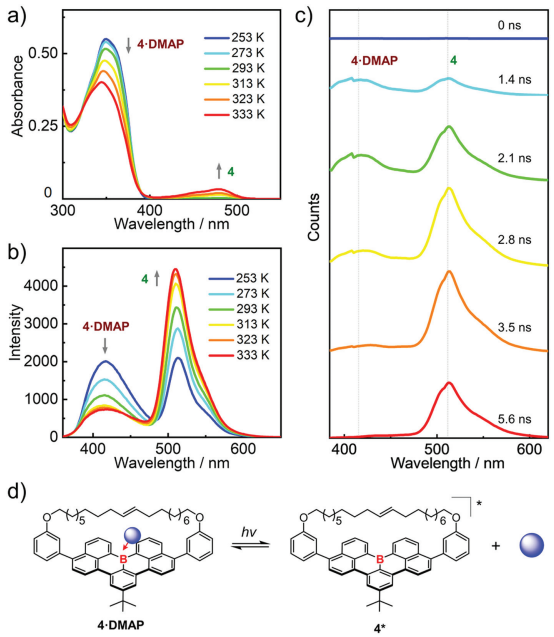

Fig. 5. Temperature-dependent (a) UV-vis absorption and (b) fluorescence spectra ($\lambda_{ex} = 350$ nm), as well as (c) time-resolved fluorescence spectra ($\lambda_{ex} = 370$ nm) of **4** (1.0×10^{-5} mol/L) in the presence of excess DMAP (2.0×10^{-4} mol/L). (d) Schematic illustration of the photodissociation of **4·DMAP**.

organoborane **4** possesses two enantiomers in one single crystal, owning to the presence of helical π-framework in its cyclic structure. Moreover, their Lewis acid-base adducts based on DMAP may dissociate in the excited state and thus display intriguing photo-responsive fluorescence properties, which can be further modulated by temperature. This study thus provides a novel design strategy for non-conjugated organoborane macrocycles, which will promote the development of stimuli-responsive macrocyclic materials with fascinating properties.

Declaration of competing interest

The authors declare that they have no known competing financial interests or personal relationships that could have appeared to influence the work reported in this paper.

Acknowledgment

This work was supported by the National Natural Science Foundation of China (Nos. 22175074, 21822507).

Supplementary materials

Supplementary material associated with this article can be found, in the online version, at doi:10.1016/j.cclet.2022.08.009.

References

[1] T.H. Shi, M.X. Wang, CCS Chem. 3 (2021) 916–931.
[2] Y. Segawa, M. Kuwayama, Y. Hijikata, et al., Science 365 (2019) 272–276.
[3] B. Hua, L. Shao, M. Li, et al., Acc. Chem. Res. 55 (2022) 1025–1034.
[4] C.F. Chen, Y. Han, Acc. Chem. Res. 51 (2018) 2093–2106.
[5] M. Mastalerz, Angew. Chem. Int. Ed. 49 (2010) 5042–5053.
[6] Z. Hassan, E. Spuling, D.M. Knoll, et al., Angew. Chem. Int. Ed. 59 (2020) 2156–2170.
[7] L. Mao, M. Zhou, X. Shi, et al., Chin. Chem. Lett. 32 (2021) 3331–3341.
[8] M. Ishida, S.J. Kim, C. Preihs, et al., Nat. Chem. 5 (2013) 15–20.
[9] M. Hirai, N. Tanaka, M. Sakai, et al., Chem. Rev. 119 (2019) 8291–8331.
[10] B.H. Di, Y.L. Chen, Chin. Chem. Lett. 29 (2018) 245–251.
[11] Y. Xu, C. Li, Z. Li, et al., CCS Chem. 3 (2021) 2077–2091.
[12] L. Yuan, J. Guo, Y. Yang, et al., CCS Chem. (2022), doi:10.31635/ccschem.022.202101738.
[13] J.M. Farrell, C. Mützel, D. Bialas, et al., J. Am. Chem. Soc. 141 (2019) 9096–9104.
[14] Y. Min, C. Dou, D. Liu, et al., J. Am. Chem. Soc. 141 (2019) 17015–17021.
[15] E.V. Grotthuss, A. John, T. Kaese, et al., Asian J. Org. Chem. 7 (2018) 37–53.
[16] L. Ji, S. Griesbeck, T.B. Marder, Chem. Sci. 8 (2017) 846–863.
[17] W.B. Lin, M. Li, L. Fang, et al., Chin. Chem. Lett. 29 (2018) 40–46.
[18] Y. Yang, J. Guo, K. Ye, et al., Mater. Chem. Front. 6 (2022) 600–606.
[19] K. Matsuo, S. Saito, S. Yamaguchi, J. Am. Chem. Soc. 136 (2014) 12580–12583.
[20] N. Ando, T. Yamada, H. Narita, et al., J. Am. Chem. Soc. 143 (2021) 9944–9951.
[21] J. Guo, Y. Yang, C. Dou, et al., J. Am. Chem. Soc. 143 (2021) 18272–18279.
[22] X. Tian, J. Guo, W. Sun, et al., Chem. Eur. J. 28 (2022) e202200045.
[23] P. Chen, R.A. Lalancette, F. Jäkle, Angew. Chem. Int. Ed. 51 (2012) 7994–7998.
[24] N. Suzuki, A. Fukazawa, K. Nagura, et al., Angew. Chem. Int. Ed. 53 (2014) 8231–8235.
[25] M. Ishida, T. Omagari, R. Hirosawa, et al., Angew. Chem. Int. Ed. 55 (2016) 12045–12049.
[26] N. Baser-Kirazli, R.A. Lalancette, F. Jäkle, Angew. Chem. Int. Ed. 59 (2020) 8689–8697.
[27] M. Chen, K.S. Unikela, R. Ramalakshmi, et al., Angew. Chem. Int. Ed. 60 (2021) 1556–1560.
[28] P. Li, D. Shimoyama, N. Zhang, et al., Angew. Chem. Int. Ed. 61 (2022) e202200612.
[29] H. Kawashima, S. Ukai, R. Nozawa, et al., J. Am. Chem. Soc. 143 (2021) 10676–10685.
[30] K. Schickedanz, T. Trageser, M. Bolte, et al., Chem. Commun. 51 (2015) 15808–15810.
[31] F. Miyamoto, S. Nakatsuka, K. Yamada, et al., Org. Lett. 17 (2015) 6158–6161.